Research Square

Preprints are preliminary reports that have not undergone peer review. They should not be considered conclusive, used to inform clinical practice, or referenced by the media as validated information.

Corallocarpus glomeruliflorus-Mediated Phyto-Fabrication of CuO Nanoparticles: Microstructural Characteristics, Optical Bandgap, and Antibacterial Activity

Mahmood Saleh

mahmoodma.chem.edu@aden-univ.net

University of Aden

Article

Keywords: Green synthesis, Corallocarpus glomeruliflorus, Copper oxide nanoparticles, characterization, Antibacterial activity

Posted Date: October 1st, 2026

DOI: https://doi.org/10.21203/rs.3.rs-10922984/v1

License: This work is licensed under a Creative Commons Attribution 4.0 International License. Read Full License

Additional Declarations: No competing interests reported.

Corallocarpus glomeruliflorus-Mediated Phyto-Fabrication of CuO Nanoparticles: Microstructural Characteristics, Optical Bandgap, and Antibacterial Activity

Mahmood Mohammed Ali Saleh
Dept, of Chemistry, Faculty of Education University of Aden, Aden, Yemen
mahmoodma.chem.edu@aden-univ.net
ORCID ID https://orcid.org/0009-0006-2098-3894.
corresponding author: mahmood0022@yahoo.com

ABSTRACT

Corallocarpus glomeruliflorus (Cucurbitaceae), an indigenous Yemeni plant, represents a previously unexplored biogenic resource for metal oxide nanoparticle synthesis. To the best of our knowledge, this study is the first to employ *C. glomeruliflorus* for the phyto-mediated synthesis of a metal oxide nanomaterial. Here, copper oxide nanoparticles (CG-CuO NPs) were synthesized using an aqueous extract of the aerial parts of *C. glomeruliflorus* and evaluated for their physicochemical and antibacterial properties. Phytochemical screening revealed phenols, alkaloids, flavonoids, anthraquinones, glycosides, saponins, terpenoids, steroids, carbohydrates, tannins, and coumarins. Nanoparticle formation and properties were investigated using UV–Vis, FTIR, XRD, SEM, and EDX analyses. The CG-CuO NPs exhibited an absorption maximum at approximately 290 nm and an optical bandgap of 3.76 eV. XRD confirmed a predominantly phase-pure monoclinic CuO structure (C2/c) with an average crystallite size of 40.97 nm. SEM revealed predominantly irregular, quasi-spherical nanoparticles (20–50 nm) with moderate agglomeration, while EDX confirmed Cu and O as the principal elemental constituents. The nanoparticles exhibited antibacterial activity against *Salmonella typhi*, *Staphylococcus aureus*, and *Escherichia coli*, with maximum inhibition zones of 20, 20, and 18 mm, respectively. These findings establish *C. glomeruliflorus* as a novel biogenic platform for CuO nanoparticle synthesis and support its potential for developing environmentally sustainable nanomaterials with antibacterial properties.

Keywords: Green synthesis; *Corallocarpus glomeruliflorus*; Copper oxide nanoparticles; characterization; Antibacterial activity;

Graphical Abstract

Green synthesis of CuO NPs using *C. glomeruliflorus* extract, including extraction, reaction with copper acetate, color change, filtration, drying, and calcination (400 °C), yielding bioactive CuO NPs with antibacterial potential.

1 Introduction

Metal oxide nanoparticles (MO NPs) have attracted increasing attention because of their distinctive physicochemical properties and broad potential applications. Plant-mediated synthesis has emerged as an alternative approach to conventional physical and chemical fabrication methods, offering the possibility of producing nanomaterials using biologically derived reagents and reducing the use of potentially hazardous chemicals[1,2]. In this approach, plant-derived metabolites can participate in the transformation of metal precursors and may contribute to nanoparticle surface stabilization, providing a biologically assisted route for nanomaterial synthesis[3]. Among MO NPs, copper oxide nanoparticles (CuO NPs) have received considerable interest because of their physicochemical properties and potential applications in heterogeneous catalysis, sensing, optoelectronics, electrochemical energy storage, agriculture, and antimicrobial technologies[4–6]. In particular, CuO NPs have demonstrated antibacterial activity against both Gram-positive and Gram-negative bacteria, including *Escherichia coli*, *Pseudomonas aeruginosa*, *Enterococcus faecalis*, *Klebsiella pneumoniae*, *Staphylococcus aureus*, and *Bacillus subtilis*[7–12]. Their biological activity, together with their semiconducting and structural properties, has therefore stimulated extensive research

into sustainable approaches for their synthesis. A growing number of plant species have consequently been explored as biogenic resources for CuO NPs synthesis. Previous studies have reported the use of extracts from *Moringa oleifera* L.[13], *Eucalyptus globulus*[14], *Aerva javanica*[15], and *Aloe vera*[16], as well as fruit-derived extracts from *Psidium guajava*[17], *Carica papaya*[18], and Punica granatum[19]. Other botanical sources, including *Camellia sinensis*[20], *Aegle marmelos*[21], and *Allium sativum*[22], have also been employed. Collectively, these studies demonstrate that plant extracts with diverse phytochemical compositions can provide useful biogenic environments for nanoparticle formation. However, the physicochemical characteristics and biological performance of phyto-synthesized nanoparticles may vary substantially with the chemical composition of the selected plant source, highlighting the importance of exploring previously uninvestigated flora. Yemen possesses a rich diversity of medicinal plants that remains comparatively underexplored as a resource for green nanotechnology. In a previous study, our group employed the Yemeni plant *Iphiona scabra* for the biogenic synthesis of zinc oxide nanoparticles (ZnO NPs), producing crystalline nanoparticles with an average size of 17.1 nm[23]. These findings support the potential of regionally available plant resources as biogenic materials for the synthesis of functional nanomaterials and provide a rationale for investigating additional Yemeni plant species. Among these plants, *Corallocarpus glomeruliflorus* (Cucurbitaceae) is an indigenous species occurring in Yemen, including the Hadramout region, where it is locally known as (Al-Madraka) or yellow roots[24–26]. Previous phytochemical investigations have demonstrated that this species contains a chemically diverse range of secondary metabolites, including steroids, terpenoids, glycosides, alkaloids, saponins, and tannins, together with appreciable phenolic and flavonoid contents[24]. These phytochemical characteristics, combined with its reported antioxidant, antibacterial, anti-inflammatory, and immunomodulatory activities[24–26], suggest that *C. glomeruliflorus* may represent a promising yet unexplored biogenic resource for nanomaterial synthesis. Despite its phytochemical richness and reported biological activities, the application of *C. glomeruliflorus* in the green synthesis of metal oxide nanoparticles has not previously been reported. To the best of our knowledge, the present study therefore represents the first investigation employing *C. glomeruliflorus* as a biogenic source for the phyto-mediated synthesis of a metal oxide nanomaterial. Here, copper oxide nanoparticles (CG-CuO NPs) were synthesized using an aqueous extract of the aerial parts of *C. glomeruliflorus*. The phytochemical composition of the extract was evaluated, and the synthesized nanoparticles were characterized using complementary physicochemical techniques to investigate their crystal structure, crystallinity, microstructural characteristics, morphology, elemental composition, and optical properties. Their antibacterial activity against selected Gram-positive and Gram-negative bacterial species was subsequently assessed. By integrating phytochemical analysis with nanoparticle synthesis, physicochemical characterization, and antibacterial evaluation, this study provides the first evidence for the potential use of *C. glomeruliflorus* in the green fabrication of CuO NPs.

2. Materials and methods

2.1. Chemicals and materials

All chemicals were used as received without further purification Copper acetate monohydrate Cu $(CH_3COO)_2.H_2O$, (99.99% purity), sodium hydroxide (NaOH, 98%), and dimethyl sulfoxide (DMSO, 99.5%) were purchased from

BDH. Deionized water (18.2 MΩ·cm resistivity) was obtained from a Millipore Milli-Q system. All other reagents were of analytical grade.

2.2. Collection and identification of *Corallocarpus glomeruliflorus* (Al-Madraka)

Fresh aerial components (stems and twigs) of *C. glomeruliflorus* Al-Madraka (Cucurbitaceae) were collected from Jabal AL-Diss Ashrqiya, Hadhramout Governorate, Yemen (14°46′10.05″ N, 49°15′59.91″ E; 117.9 m above sea level) on 30 August 2023. The plant was taxonomically identified by Prof. Othman Saad Saeed Al-Hawshabi at the Botany Department, Faculty of Science, University of Aden, Yemen. A voucher specimen (No. CG-2022-001) was deposited in the herbarium of the same department for future reference.

2.3. Preparation of *Corallocarpus glomeruliflorus* (Al-Madraka) Extract

The plant materials were cut into smaller segments and allowed to dry naturally in shaded conditions at ambient temperature. A mechanical grinder was employed to process the dried material into a uniform powder, which was then stored in airtight containers until further analysis. The extraction process utilized 20 g of powdered *C. glomeruliflorus* (Al-Madraka) combined with 100 mL, the mixture was heated to 80 ^{0}C for 60 min on a magnetic stirrer with continuous stirring according to the method of [23]. The solution turned pale brown. The resulting extract was then filtered and cooled to room temperature (RT). In order to use the extract to create CuO NPs, it was finally cooled and maintained at 4°C, Fig. 1 shows a pictorial representation of the *C. glomeruliflorus* extract production process.

Fig 1. Preparation mechanism of *C. glomeruliflorus* extract.

2.4. Biosynthesis of CuO NPs

Copper oxide nanoparticles (CG-CuO NPs) were synthesized via a green route following the methodology optimized in our previous work [23], with minor modifications. Briefly, (10 ml) of the aqueous *C. glomeruliflorus* extract was mixed with (190 ml) of an aqueous copper acetate monohydrate solution (0.1M). The reaction mixture was kept under continuous magnetic stirring at ambient temperature. Within a few minutes of mixing, a prominent visual color change was observed, shifting from a pale blue precursor solution to a dark green hue. Subsequently, the pH of the mixture was adjusted to 7.5 by the drop wise addition of (0.1M) sodium hydroxide (NaOH), which immediately triggered a transition into a jet-black turbid suspension, signaling the rapid nucleation of amorphous copper hydroxide intermediates. A comparable color transformation upon adding plant extract to copper precursors has been previously documented [27,28]. The resulting suspension was incubated at 80°C under constant magnetic stirring for 90 min to promote nanoparticle growth. After cooling to room temperature, the colloidal suspension was harvested by centrifugation at 3000 rpm for 10 min. The recovered precipitate was thoroughly washed three times with deionized water and absolute ethanol to remove unreacted precursors and organic residues. The purified pellet was dried in a hot air oven at 50°C for 24 h and subsequently calcined at 400°C for 2 h to yield highly crystalline, jet-black CuO NPs. This calcination profile 400°C aligns with thermal annealing parameters previously reported for optimal phase formation [29]. The overall green synthesis workflow of the CG-CuO NPs is schematically illustrated in Fig 2.

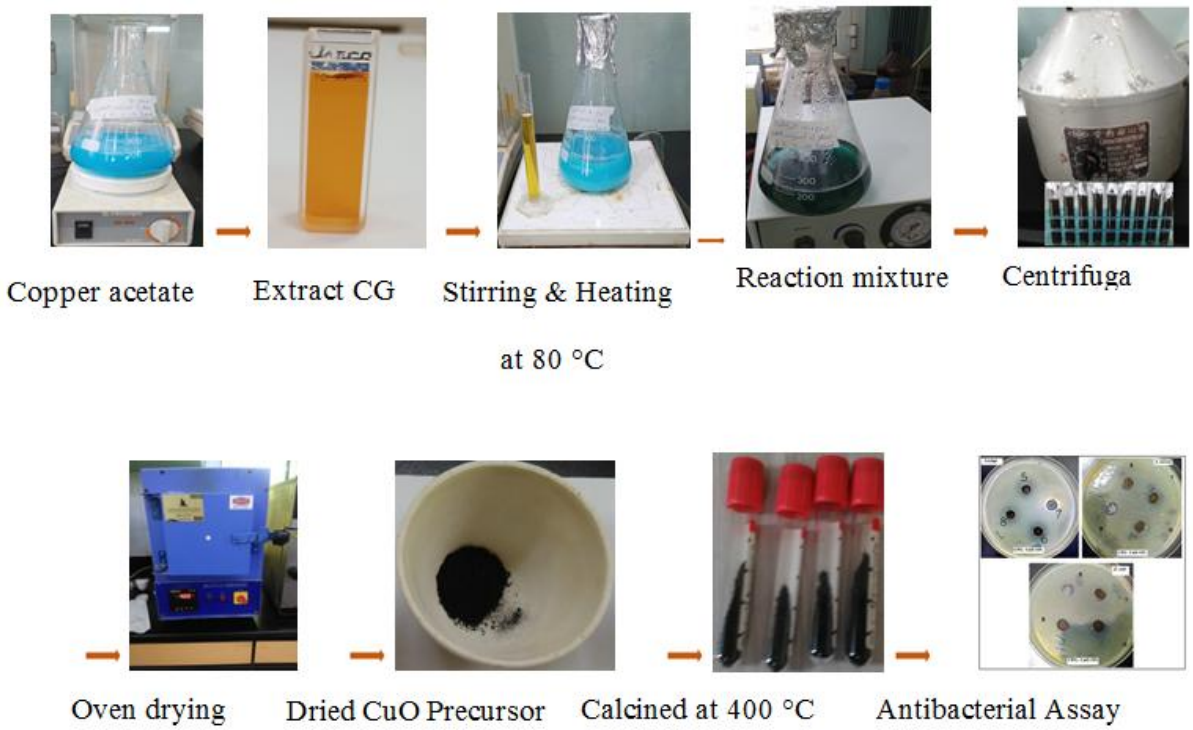

Fig. 2 Green synthesis of CuO NPs using *C. glomeruliflorus* extract

2.4.1. Mechanism of green synthesis of CuO NPs using *C. glomeruliflorus* extract

The biosynthesis of CuO NPs using *C. glomeruliflorus* extract involves a sequence of physicochemical and thermal processes mediated by phytochemicals. The extract contains a diverse array of bioactive compounds, including phenols, alkaloids, flavonoids, anthraquinones, glycosides, saponins, terpenoids, steroids, carbohydrates, tannins, and coumarins. These molecules possess functional groups (–OH, C=O, C–O, C=N, –COOH, etc.) capable of coordinating with Cu^{2+} ions. Upon mixing the extract with copper acetate monohydrate, phytochemicals chelate Cu^{2+} ions, forming metal–phytochemical complexes. Adjustment of the pH to 7.5 with NaOH promotes the hydrolysis of copper species and the precipitation of copper hydroxide basic copper compounds, yielding a black turbid suspension. Phytochemicals adsorb onto the surfaces of nuclei as capping agents, regulating nucleation and inhibiting agglomeration. Subsequent heating at 80 °C for 90 min under stirring facilitates precursor maturation and controlled growth, while maintaining colloidal stability. The collected precursor is then dried and calcined at 400 °C for 2 h. During calcination, organic constituents are decomposed, and the copper hydroxide precursor undergoes thermal decomposition and reorganization to yield crystalline CuO NPs. The size, morphology, crystallinity, and yield of CuO NPs are strongly influenced by the concentration and nature of phytochemicals, pH, temperature, reaction time, copper precursor concentration, and the extract-to-precursor ratio. In agreement with the general framework proposed by *Aleman-Ramirez* et al. [30], the process can be considered in terms of activation/complexation, nucleation and growth, and stabilization/termination stages. Overall, the synergistic action of *C. glomeruliflorus* phytochemicals, alkaline conditions, controlled heating, and calcination enables the efficient formation of crystalline (CG-CuO NPs) through a simple, eco-friendly route. The proposed mechanism is schematically illustrated in Fig. 3.

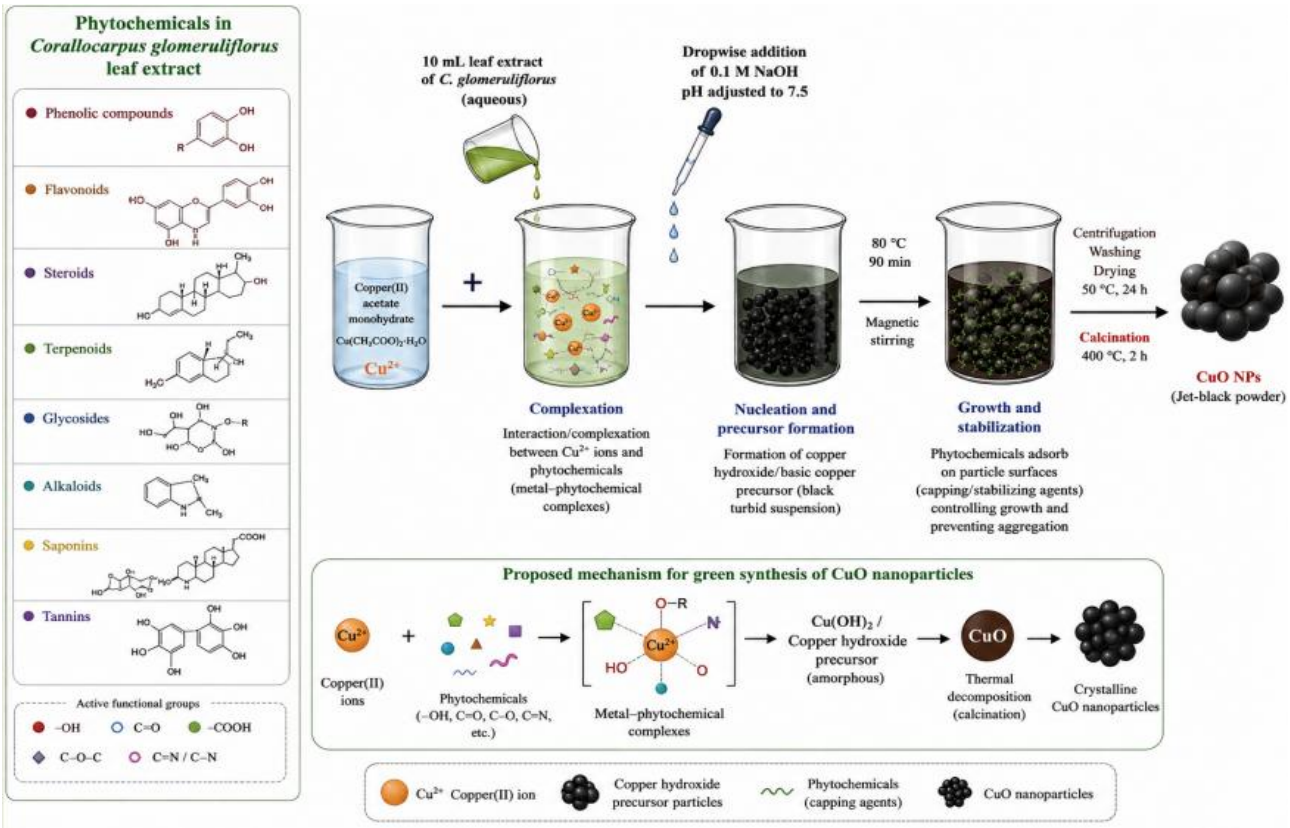

Fig. 3 Mechanism for the synthesis of CuO NPs using *C. glomeruliflorus* extract**.**

2.5. Characterization of the CuONPs

2.5.1. Ultraviolet–Visible (UV–Vis) spectroscopy

The optical properties of both the aqueous extract of *C. glomeruliflorus (Al-Madraka)* and the green-synthesized CG-CuO NPs were investigated using Ultraviolet–Visible (UV–Vis) spectroscopy. To evaluate the nanostructures, 0.05mg of the fabricated ZnO nanopowder was thoroughly dispersed in 4ml of deionized water and subjected to ultrasonication for 15 min to attain a highly homogeneous colloidal suspension. The spectrophotometric analyses were executed using a Jasco V-730 UV-Visible spectrophotometer (JASCO Corporation, Tokyo, Japan; Serial No. A063361798). The electronic absorption spectra were systematically recorded across a scanning wavelength range of 200–900 nm.

2.5.2. Fourier transform infra‑red (FT‑IR) spectroscopy

FT-IR analysis was employed using (Alpha,Bruker, Germany). The aqueous extract of *C. glomeruliflorus* (Al-Madraka) and the CG-CuONPs, were scanned in the spectral array from 450 to 4000 cm^{-1} at 4 cm^{-1} resolutions and different spectra were obtained to determine the functional groups involved in the synthesis of CG-CuONPs and aqueous leaf extract.

2.5.3. X-ray diffraction

The X-Ray powder diffraction technique was used to investigate the crystalline structure, size and formation of the compounds. CuO NPs which were synthesized via the green route using *C. glomeruliflorus (Al-Madraka)* extract were analyzed using single crystal X-Ray Diffractometer (Bruker D8 Discover Germany) with Cu-Kα radiation (λ = 1.54060 Å). The scanning was done in the region of 2θ from 20° to 80°.

2.5.4. SEM- EDX analysis

Surface morphology and actual particle size of the prepared CuO NPs was determined using SEM machine (EM (NOVA FEISEM-450 applied with EDX detector, Germany). The EDX function was also embedded in the SEM. The prepared CG-CuONPs samples were placed into SEM machine and subjected to 10 kV voltage, images at 50 kx magnification were taken. The elemental analysis of asynthesized *C. glomeruliflorus (Al-Madraka)* mediated NPs were employed through Energy Dispersive X-ray (EDX) spectroscopy and elemental composition was determined.

2.5.4. Scanning electron microscopy (SEM)

The morphology of the CG-CuONPs was examined using TESCAN Ultra-High Resolution and SEM (Germany). An X-ray energy dispersive spectroscope (EDS) was used with a scanning electron microscope (20 kV). The nanoparticles were dispersed in DMSO and, sonicated for 20 min, and one drop was placed on a copper grid coated with carbon to prepare the samples. Prior to examination, the samples were vacuum-dried for 24 h at an accelerating voltage of 15 kV. Thise method allows for extensive structural analysis of the nanoparticles by providing high-resolution imaging capabilities of 1 nm at accelerating voltage of 15 kV.

2.6. Antibacterial activity evaluation

2.6.1 Bacterial strains and inoculum preparation

The National Center for Central Public Health Laboratories (Mukalla, Hadramout, Yemen) provided bacterial a panel of pathogenic bacterial strains, including Grampositive bacteria (*S. aureus*) and two Gram-negative bacteria (*E. coli*, and *S. typhi*) strains to evaluate the antimicrobial properties of CG-CuO NPs. All bacterial cultures were maintained on nutrient agar slants at 36 ◦C. Fresh cultures were prepared by inoculating a single colony into MHB and incubating overnight at 37 ◦C on an orbital shaker. The bacterial suspensions were adjusted to a 0.5 McFarland standard (~1.5 × 108 CFU/mL) prior to use [31].

2.6.2. Agar well diffusion assay

The antibacterial activity was assessed using the agar well diffusion method. MHA plates were swabbed uniformly with 100 µL of each bacterial suspension. Wells of 6 mm diameter were punched into the agar using a sterile cork borer. The wells were filled with CG-CuO NPs (2.5, 5, 10 and 20 mg/mL), while (DSMO) as a standard reference. The inhibitory zones (IZ) were measured after 24 h of incubation at 37 ◦C.

3. Results and Discussion

3.1. Characterization of copper oxide nanoparticles (CuO NPs)

3.1.1. Visual observation

Initially of the synthesis, the precursor copper acetate was completely dissolved in deionized water (DW), yielding formed a pale blue solution. Upon the introduction of the *C. glomeruliflorus* (Al-Madraka) extract into the precursor solution, a rapid and distinct color transition was observed within a few minutes. This immediate chromatic shift served as the primary macroscopic indicator confirming the initiation of copper oxide nanoparticle (CG-CuO NPs). To drive the reaction to completion, the mixture was thermally treated at 80°C for 90 min. Throughout this process, the solution exhibited a sequential transformation, changing from pale blue solution to a stable dark green, and ultimately stabilizing as a dense, stable dark green/brown suspension. This characteristic visual transition definitively indicates the successful formation of CuO NPs, mediated by the active phytoconstituents within the extract. Specifically, flavonoids and phenolic compounds present in the *C. glomeruliflorus* (Al-Madraka) extract are highly expected to act as the principal reducing and capping agents, facilitating the bioreduction of Cu^{2+} ions into stable CG-CuO NPs. This chromatic change confirms the reduction of Cu^{2+} ions and the formation of stabilized CG-CuO NPs, where the plant's phytochemicals served as both reducing and capping agents. The chronological stages of this visual transformation are clearly illustrated in Fig. 4(a, b, c) [31].

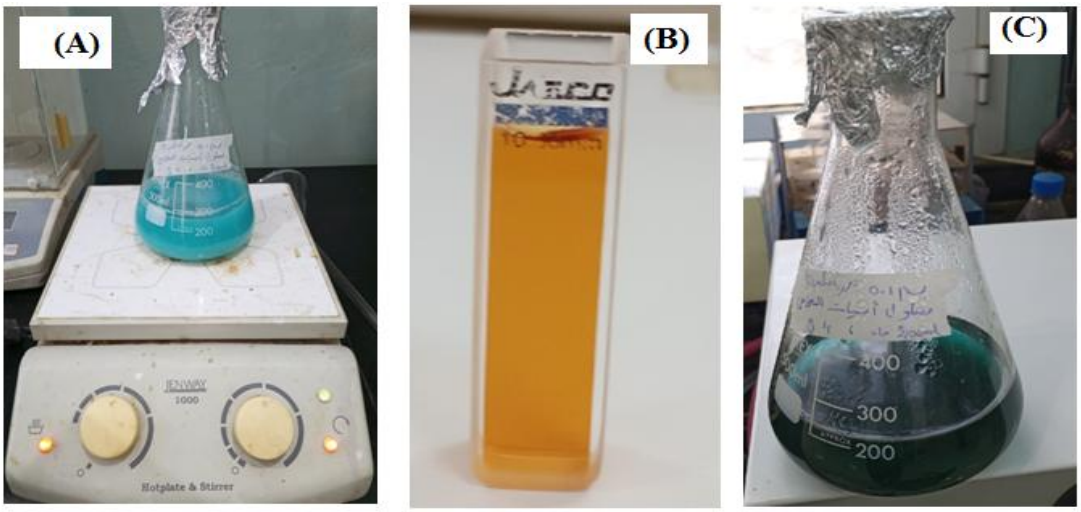

Fig 4. Color of (A) copper acetaet monehydrate solution, (B) when *C. glomeruliflorus* extract was added, (C) color shifted at PH (7.5).

3.1.2.Phytochemical analysis of *C. glomeruliflorus* extract

Preliminary phytochemical screening of the *C. glomeruliflorus* aqueous extract confirmed the rich presence of key bioactive secondary metabolites, including phenols, alkaloids, flavonoids, anthraquinones, glycosides, saponins, terpenoids, steroids, carbohydrates, tannins, and coumarins, were absent (Table 1). These qualitative findings are in strong agreement with prior detailed spectroscopic and chromatographic characterizations of the plant material. Bin-Asal et al.[24] elucidated the complex chemical profiling of the extract using High-Performance Liquid Chromatography coupled with Quadrupole Time-of-Flight Tandem Mass Spectrometry (HPLC–QTOF-MS/MS; Agilent 1200 HPLC / Agilent 6550 QTOF-MS/MS), tentatively identifying several major polyphenolic and terpenoid constituents, such as maritimetin, assafoetidin, kaempferol 3-rhamnoside 7-xyloside, and lespenefril [24]. Furthermore, Gas Chromatography–Mass Spectrometry (GC–MS) analyses by Ododo et al. [32] corroborated the high content of phenolic compounds, flavonoids, tannins, sterols, and essential fatty acids (mainly oleic acid and linoelaidic acid), alongside primary metabolites like proteins and carbohydrates. The presence of these phytoconstituents particularly electron-rich phenolic and polyphenolic entities suggested their primary role as natural reducing, capping, and stabilizing agents during the bio-reduction of copper ions into CuO NPs (CuO NPs) [29]. To validate this hypothesis, subsequent Fourier-Transform Infrared Spectroscopy (FTIR) analysis was conducted, which unequivocally confirmed the participation and transformations of these oxygen-containing functional groups in the nucleation, surface passivation, and stabilization of the synthesized CuO NPs.

Constituent	Reagent Test	Positive Result Indicator	Observation
Alkaloids	Mayer's test	Creamy precipitate	++
	Wagner's test	Reddish-brown precipitate	+++
	Dragendorff's test	Red precipitate	+++
Anthraquinones	Modified Bornträger's test	Pink/red or violet color in lower phase	+++
Flavonoids	Shinoda test	Pink scarlet coloration	+++
	C_2H_5OH / KOH test	Yellow color	+++
Glycosides	Keller-Kiliani test	Reddish-brown coloration	+++
Saponins	Foam test	Persistent foam (10 min)	+++
Terpenoids	Salkowski test	Reddish-brown coloration	+++
Steroids	Liebermann-Burchard test	Greenish color	++
Carbohydrates	Fehling's test	Reddish precipitate	+++
	Molisch's test	Reddish-violet colored ring	+++
	Benedict's test	Reddish precipitate	+++
Tannins	Ferric chloride ($FeCl_3$)	Blackish-blue color	-
	Lead acetate test	Yellowish-white precipitate	+++
Phenols	Ethanol + $FeCl_3$ (pinch)	Greenish-yellow color	+++
	1% $FeCl_3$ + Potassium ferrocyanide	Greenish-blue color	+++
Coumarins	10% NaOH test	Yellow color	+++

Table 1. Preliminary phytochemical constituent in aqueous extract of *C. glomeruliflorus*. Key − absent + present.

3.1.2. UV–Visible analysis of the CuO NPs

The green synthesis of copper oxide nanoparticles (CG-CuONPs) using *C. glomeruliflorus* (Al-Madraka) extract was confirmed by UV–Vis spectroscopy over the wavelength range of 200–900 nm. The UV–Vis spectrum of the pure plant extract Fig. 5a exhibited two characteristic absorption bands at 240.2 nm and 412.6 nm, which are attributed to the presence of bioactive phytochemicals such as flavonoids and phenolic compounds. These compounds play a vital role as both reducing and stabilizing (capping) agents during nanoparticle formation [9]. Fig. 5b illustrates the absorption spectrum of the synthesized CG-CuONPs using copper acetate monohydrate ($Cu(CH_3COO)_2 \cdot H_2O$) as a precursor. A prominent absorption peak was observed at 290 nm, confirming the successful formation of CuO NPs. This result is consistent with previous studies, where CuO nanoparticles synthesized using *Beta vulgaris* extract exhibited a similar absorption peak around 275 nm [3]. The optical band gap energy of the synthesized CG-CuONPs was estimated using the Tauc relation:

$$(\alpha hv)2 = A(hv - Eg)$$

The Tauc plot Fig. 5c yielded a band gap value of 3.76 eV, which is higher than that of bulk CuO (1.2–1.9 eV), indicating a noticeable blue shift. This shift can be attributed to the quantum confinement effect resulting from the reduced particle size at the nanoscale. In addition, surface defects, lattice strain, and oxygen vacancies may contribute to the modification of the electronic structure. The relatively high band gap value (3.76 eV) further confirms the nanoscale nature of the synthesized particles, which is in good agreement with the crystallographic findings obtained from XRD analysis. Comparable results have been reported in the literature. For instance, CuO nanoparticles synthesized using *T. aestivum* leaf extract exhibited an absorption peak at 305 nm with an optical band gap energy (Eg) of 4.13 eV [33], while Tithonia diversifolia-mediated synthesis showed a peak around 265 nm [34]. Similarly, CuO nanoparticles synthesized using *L. pruinosum* extract displayed an absorption band at 375 nm [35] 275 nm [3] and 288 nm [36]. We have previously reported an absorption peak of 373 nm for *I. scabra* in our earlier study [23,37,38]. These variations in absorption behavior are mainly attributed to differences in synthesis routes, phytochemical composition, and particle size distribution.

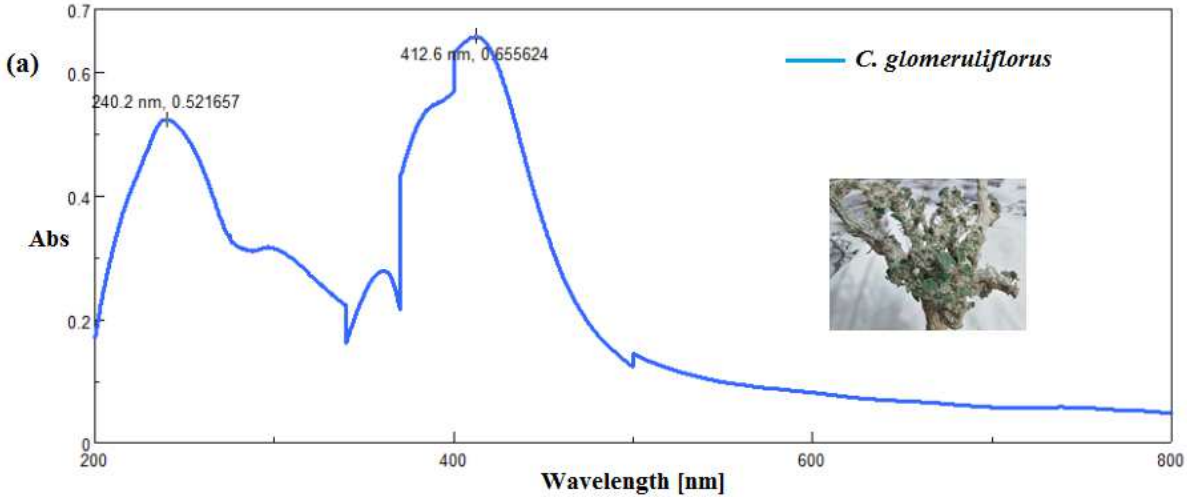
(a)
C. glomeruliflorus
240.2 nm, 0.521657
412.6 nm, 0.655624
Abs
Wavelength [nm]

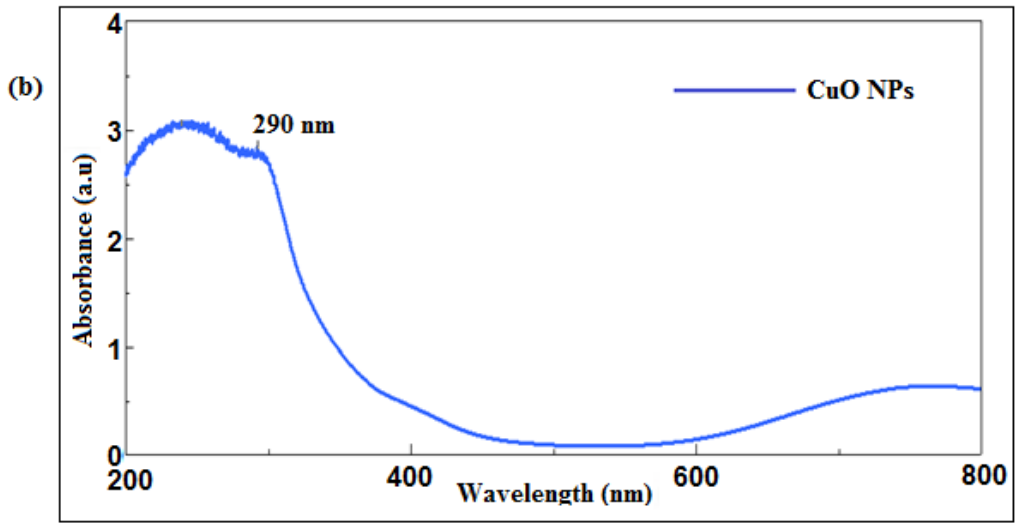
(b)
CuO NPs
290 nm
Absorbance (a.u)
Wavelength (nm)

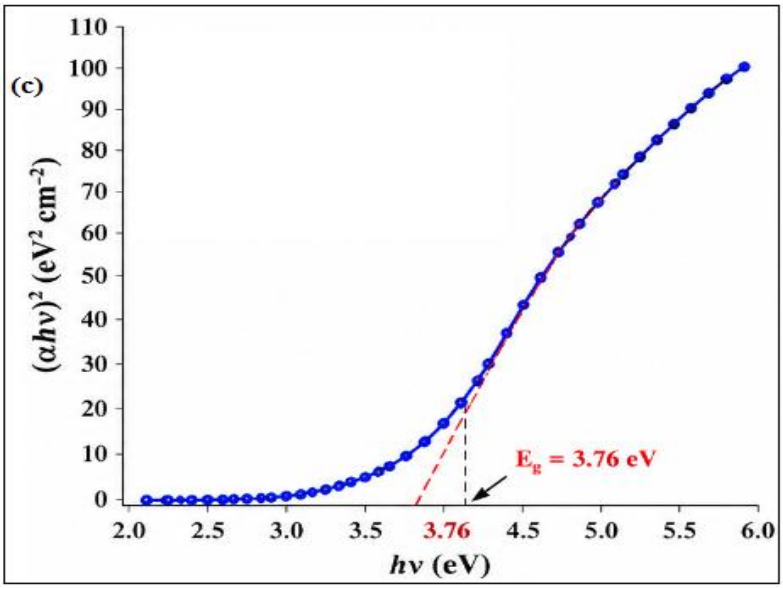
(c)
$(\alpha h\nu)^2$ (eV^2 cm^{-2})
E_g = 3.76 eV
$h\nu$ (eV)

Fig. 5. UV-Vis absorption of spectra of *C. glomeruliflorus* extract (a), CuONPs from *C. glomeruliflorus* plant (b) and (c) Tauc plot of CuO NPs.

3.1.3. FT-IR spectroscopy analysis

Fourier-transform infrared (FT-IR) spectroscopy was used to identify the principal functional groups present in *C. glomeruliflorus* powder and to investigate the surface chemical changes associated with the biosynthesis of copper oxide nanoparticles (CG-CuO NPs). The FT-IR spectra of the plant powder and the synthesized CuO NPs are presented in Figs. 6 and 7, respectively. The FT-IR spectrum of *C. glomeruliflorus* powder exhibited characteristic bands at 3280.95, 2918.04, 1413.64, 1031.32, 854.67, and 712.34 cm^{-1} [23, 37]. The broad band centered at 3280.95 cm^{-1} can be attributed to O–H stretching vibrations, indicating the presence of hydroxyl-containing constituents, such as phenolic compounds and alcohols. The band at 2918.04 cm^{-1} is consistent with aliphatic C–H stretching vibrations. The bands around 1413.64 and 1031.32 cm^{-1} fall within the fingerprint region and can be associated with bending and C–O-containing vibrations of plant-derived organic constituents. The lower-wavenumber bands at 854.67 and 712.34 cm^{-1} may be related to out-of-plane or skeletal vibrations of organic compounds. Such spectral features are consistent with the complex phytochemical composition expected for plant biomass. Following the biosynthesis of CG-CuO NPs, noticeable changes in both the position and intensity of the FT-IR bands were observed. The synthesized CG-CuO NPs exhibited bands at approximately 3227.75, 2981.59, 1566.55, 1492.41, 1398.06, 1150, 1022.55, 673.39, 585.18, and 475.22 cm^{-1}. The broad band at 3227.75 cm^{-1} is attributable to O–H stretching, most likely associated with surface hydroxyl groups and/or adsorbed moisture. The band near 2981.59 cm^{-1} can be assigned to aliphatic C–H stretching. The bands in the 1566–1398 cm^{-1} region are associated with vibrations of residual oxygen-containing organic constituents and/or bending modes of surface-bound species. Similarly, the bands near 1150 and 1022.55 cm^{-1} are located in the fingerprint region and may be related to C–O and/or C–N vibrations originating from phytochemical residues on the nanoparticle surface. Similar retention of plant-derived functional groups after green synthesis has been reported for plant-mediated CuO NPs and is generally interpreted as evidence for the involvement of phytochemicals in nanoparticle formation and surface stabilization. Most importantly, the appearance of distinct bands at 673.39, 585.18, and 475.22 cm^{-1} provides strong spectroscopic evidence for Cu–O lattice vibrations. Vibrational bands in the low-wavenumber region, particularly approximately 400–700 cm^{-1}, are widely reported for Cu–O stretching modes in CuO and are therefore consistent with the formation of the CuO phase. The comparison between the plant powder and CG-CuO NPs therefore demonstrates a clear modification of the original phytochemical fingerprint together with the emergence of characteristic low-frequency Cu–O vibrations. These changes suggest that plant-derived biomolecules participated in the biosynthesis process and remained associated, at least partially, with the nanoparticle surface, while the low-wavenumber bands support the formation of CuO. This interpretation is consistent with the proposed role of plant phytochemicals as reducing, coordinating, and/or capping agents during plant-mediated CG-CuO NPs synthesis [38,37-44].

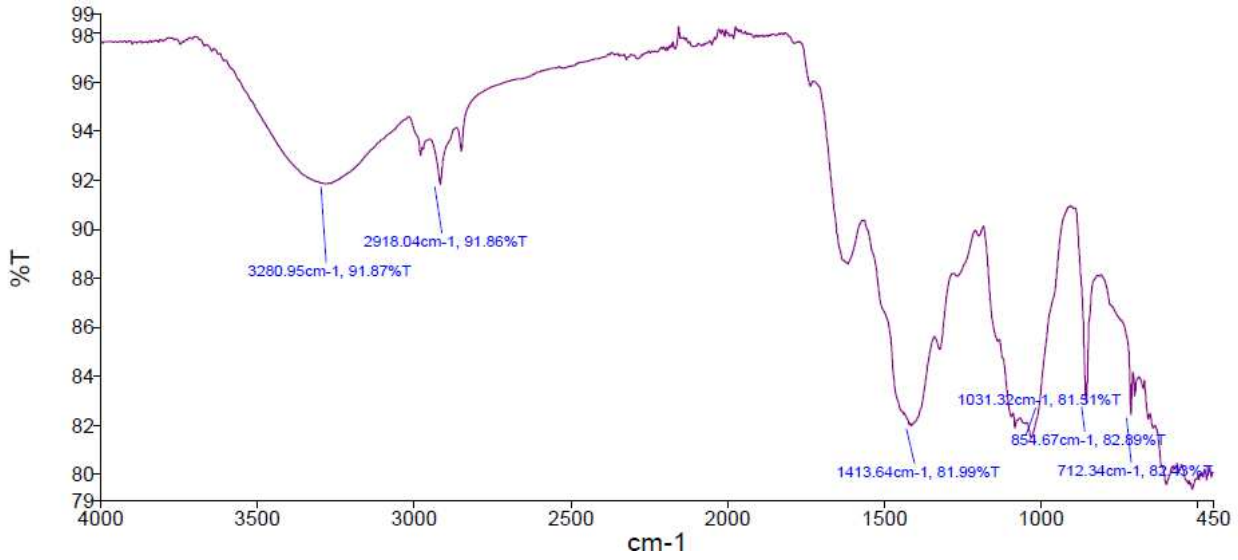

Fig. 6 FT-IR spectra of *C. glomeruliflorus* powder.

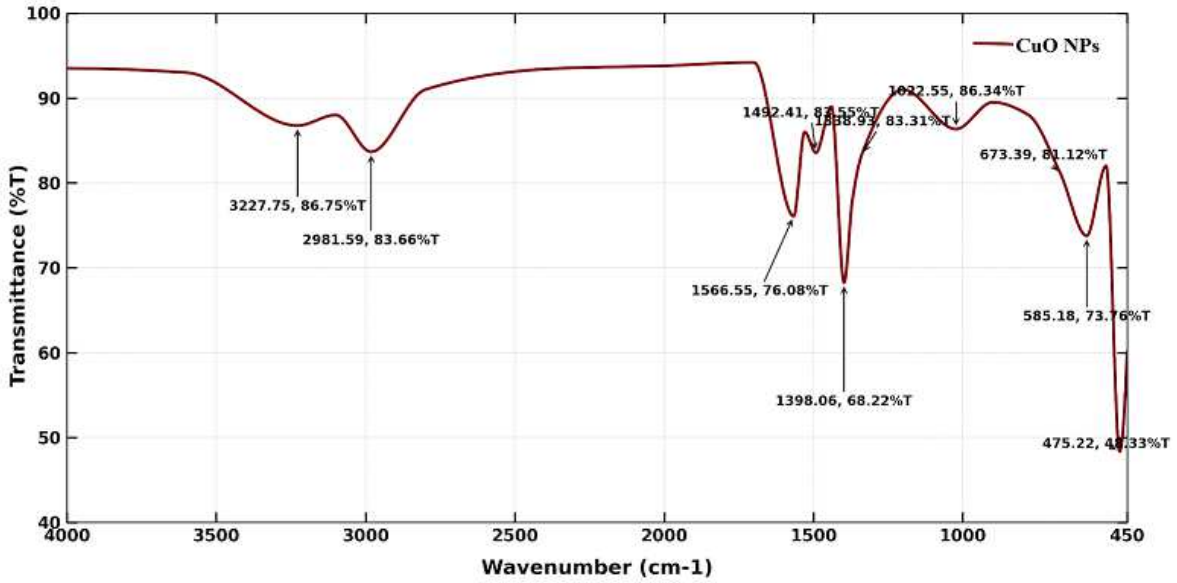

Fig.7 FT-IR spectra of CuO NPs synthesized using *C. glomeruliflorus*.

3.1.4. XRD analysis

The crystalline structure and phase composition of the biosynthesized copper oxide nanoparticles (CG-CuO NPs) were investigated by X-ray diffraction (XRD), and the resulting diffraction pattern is presented in Fig. 8. Eleven well-defined diffraction reflections were observed at 2θ values of 32.54°, 35.55°, 38.72°, 48.78°, 53.55°, 58.21°,

61.55°, 66.26°, 68.12°, 72.35°, and 75.14°. These reflections were indexed to the (110), (−111), (111), (−202), (020), (202), (−113), (−311), (220), (311), and (−222) crystallographic planes, respectively, which reveals the monoclinic structure of CuO with space group C2/c (JCPDS card no. 00–048-1548, Tenorite-C2/c). These patterns are in good agreement with the earlier studies on the green synthesis of CuO NPs [23,28,29,43]. No additional diffraction reflections attributable to crystalline secondary phases were detected within the resolution and detection limit of the XRD measurement. Accordingly, the pattern supports the formation of predominantly phase-pure monoclinic CuO rather than proving absolute chemical purity. The relatively sharp and well-resolved reflections indicate a good degree of crystallinity and the presence of coherent crystalline domains at the nanoscale. The monoclinic CuO structure is described by the lattice parameters a = 4.653 Å, b = 3.410 Å, c = 5.108 Å, and β = 99.48°, which are consistent with reported crystallographic parameters for monoclinic CuO. The crystallite size (D) was calculated for each indexed diffraction peak using the Debye–Scherrer Eq. (1) [23, 31,44], as shown below.

$$D = \frac{K\lambda}{\beta Cos\theta} \quad (1)$$

where D is the crystallite size (nm), K is the Scherrer shape factor (0.94), λ is the wavelength of Cu Kα radiation (0.15406 nm), β is the full width at half maximum (FWHM) expressed in radians, and θ is the Bragg diffraction angle.

To further evaluate the structural quality of the synthesized CuO NPs, the lattice microstrain (ε) was determined using Eq. (2).

$$\varepsilon = \frac{\beta}{4\tan\theta} \quad (2)$$

where β represents the FWHM (radian) and θ is the Bragg diffraction angle.

The dislocation density (δ), which reflects the concentration of crystallographic defects within the crystal lattice, was estimated using the following relationship Eq. (3) [23,31].

$$\delta = \frac{1}{D^2} \quad (3)$$

where D is the crystallite size calculated from the Debye–Scherrer equation.

The calculated crystallite size (D), lattice microstrain (ε), and dislocation density (δ) for all diffraction peaks are summarized in Table 2. The calculated crystallite sizes ranged from 35.98 to 44.12 nm, with an average value of 40.97 nm. The mean microstrain and dislocation density were 2.00×10^{-3} and 0.603×10^{-3} nm^{-2}, respectively, indicating relatively low lattice distortion and defect density in the synthesized CG-CuO NPs. The dislocation density (δ) exhibits an inverse relationship with the crystallite size (D), where δ decreases as D increases, following the relation $\delta = 1/D^2$. These results indicate the formation of phase-pure, well-crystallized CuO NPs with low structural defects through the green synthesis route. Overall, the XRD results demonstrate that the green synthesis using *C. glomeruliflorus* extract produced predominantly phase-pure monoclinic CuO with well-defined crystallinity, crystallite dimensions in the nanometer range, and relatively low lattice microstrain and dislocation

density. The obtained crystallite size is also comparable to those reported for CuO NPs synthesized through other plant-mediated approaches [40-44] and in CuO NPs synthesized using *A.auriculiformi, I.chinesis*, *B.sapida*, *M.oleifera* and *B.gibsonnii* indicating that the present biosynthetic route is capable of producing structurally well-defined CuO nanocrystalline material.

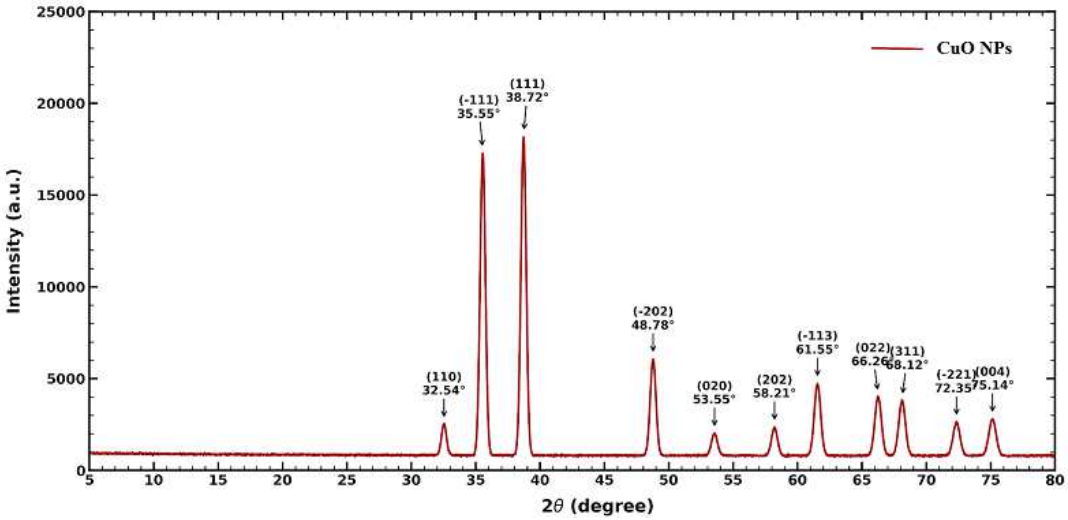

Fig. 8 XRD of extract *C. glomeruliflorus* synthesized CG-CuONPs.

No.	2θ (°)	FWHM (°)	(hkl)	d (nm)	D (nm)	ε (×10⁻³)	δ (×10⁻³ nm⁻²)
1	32.54	0.230	(110)	0.2749	35.98	3.44	0.772
2	35.55	0.227	(-111)	0.2523	36.75	3.09	0.740
3	38.72	0.205	(111)	0.2324	41.08	2.55	0.593
4	48.78	0.221	(-202)	0.1865	39.47	2.13	0.642
5	53.55	0.221	(020)	0.1710	40.26	1.91	0.617
6	58.21	0.211	(202)	0.1584	43.09	1.65	0.539
7	61.55	0.218	(-113)	0.1505	42.41	1.60	0.556
8	66.26	0.215	(022)	0.1409	44.12	1.44	0.514
9	68.12	0.223	(311)	0.1375	43.00	1.44	0.541
10	72.35	0.232	(-221)	0.1305	42.42	1.38	0.556
11	75.14	0.238	(004)	0.1263	42.11	1.35	0.564
Mean					**40.97**	**2.00**	**0.603**

Table 2. XRD data and calculation of the average size of synthesized CG-CuO NPs.

3.1.5. SEM - EDX analysis

The surface morphology of the green-synthesized copper oxide (CG-CuO NPs) nanoparticles was examined using Scanning Electron Microscopy (SEM). As illustrated in the SEM micrograph in Fig 9, the sample exhibits a revealed are predominantly irregular, quasi‑spherical, with sizes in the 20–50 nm range and a moderate tendency to agglomerate, the primary particle size is consistent with XRD size, consistent with similar findings reported by [45].

SEM analysis clearly indicates that phytochemicals present in the *C. glomeruliflorus* extract (e.g., flavonoids, phenols) play a crucial role as reducing and stabilizing agents in the formation of the CuO nanostructure. Similar CuO nanostructures have been reported in the literature using various plant extracts [46]. Although TEM analysis was not available in this study, the crystallite size was accurately determined from XRD using the Scherrer equation (40.97 nm). The observed morphology, combined with the XRD results, confirms the nanoscale nature of the synthesized CuO NPs. Compositional analysis was performed via EDS, as shown in the corresponding spectrum Fig. 10. The spectrum confirms that the nanomaterial is composed primarily of copper (Cu) and oxygen (O), with no detectable inorganic impurities. The characteristic peaks for copper (Cu) were identified at approximately 0.93 keV, 8.04 keV, and 8.90 keV, whereas the oxygen (O) peak was observed at approximately 0.52 keV. Quantitative analysis revealed elemental compositions of approximately 82.8 wt% copper and 17.2 wt% oxygen, showing a slight deviation (~2.91%) from the theoretical stoichiometry of pure CuO (79.89 wt% Cu and 20.11 wt% O). The corresponding atomic percentages were calculated as 54.79 % Cu and 45.21% O, closely approaching the ideal 1:1 atomic ratio of CuO. This minor variance falls well within the permissible instrumental tolerance (±1–3%) for semi-quantitative EDX analysis of light elements, confirming the successful synthesis of high-purity CuO NPs. Furthermore, the trace carbon signal in the spectrum originates from residual capping phytochemicals from the *C. glomeruliflorus* extract, as well as atmospheric CO_2 adsorption or the carbon tape used in sample preparation [37, 40–44].

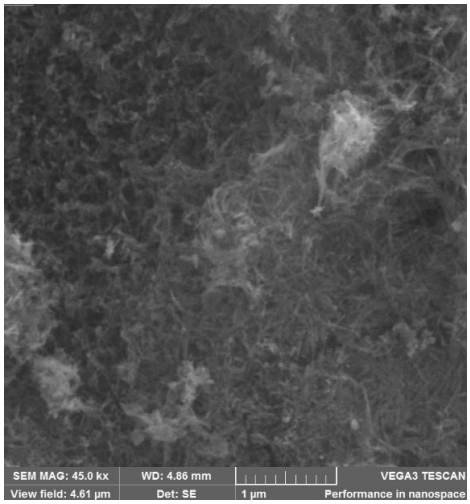

Fig. 9 SEM micrograph of CuONPs using *C. glomeruliflorus* extract.

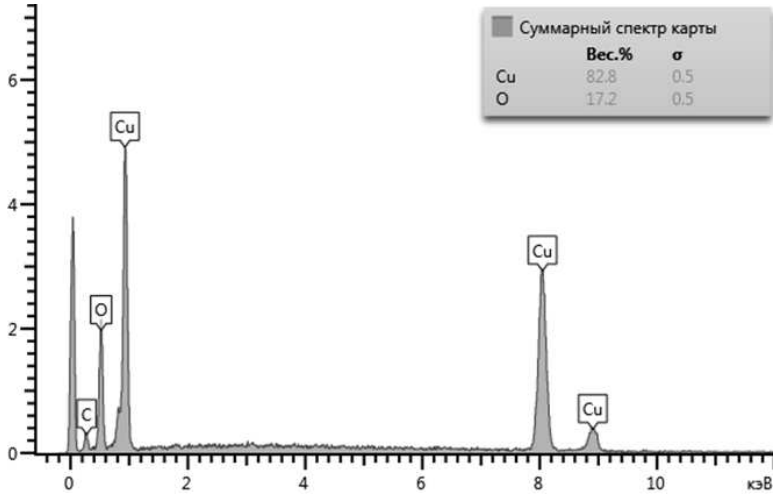

Fig. 10 EDX micrograph spectrum of CuONPs using *C. glomeruliflorus* extract.

4. Antibacterial activity of *C. glomeruliflorus* extract mediated CuO NPs

The antibacterial activity of the biosynthesized CG-CuO NPs was evaluated against *Salmonella typhi*, *Staphylococcus aureus*, and *Escherichia coli* using the agar well diffusion method at concentrations of 2.5, 5, 10, and 20 mg/mL. The inhibition zone diameters obtained for the tested bacterial strains are presented in Table 3 and Fig 11. The CG-CuO NPs exhibited clear antibacterial activity against all tested microorganisms, with the magnitude of inhibition varying among the bacterial strains and nanoparticle concentrations. *S. typhi* exhibited a consistently high susceptibility, with an inhibition zone diameter of 20 mm at all tested concentrations. *S. aureus* showed inhibition zones of 18, 20, 18, and 20 mm at concentrations of 2.5, 5, 10, and 20 mg/mL, respectively. In comparison, *E. coli* exhibited inhibition zones of 14, 18, 11, and 15 mm at the corresponding concentrations, indicating comparatively lower susceptibility. The antibacterial activity of CG-CuO NPs may be associated with the combined effects of several physicochemical mechanisms, including interactions between the nanoparticle surface and bacterial cell envelopes, the release of Cu^{2+} ions, generation of reactive oxygen species (ROS), and subsequent oxidative damage to cellular components. These effects may compromise bacterial membrane integrity and interfere with essential cellular processes, ultimately resulting in bacterial growth inhibition and cell death. However, the relative contribution of these mechanisms was not directly investigated in the present study and therefore requires experimental verification. The differences in antibacterial susceptibility among the tested bacterial strains may be related to variations in their cell envelope structure, membrane composition, and interactions with CuO nanoparticles. The relatively higher inhibition observed for *S. typhi* and *S. aureus* compared with *E. coli* may reflect differences in bacterial surface characteristics and nanoparticle–cell interactions. Nevertheless, the absence of a consistent increase in inhibition zone diameter with increasing nanoparticle concentration suggests that the antibacterial response was not strictly concentration-dependent under the experimental conditions used in this study. The observed antibacterial activity is consistent with previous reports describing the antimicrobial potential of plant-mediated CuO NPs against both Gram-positive and Gram-negative pathogenic bacteria [40–42,46]. Overall, the results

demonstrate that the green-synthesized CG-CuO NPs possess appreciable antibacterial activity against the tested bacterial strains, with maximum inhibition zones of 20 mm for *S. typhi* and *S. aureus* and 18 mm for *E. coli*. These findings support the potential of *C. glomeruliflorus*-mediated CG-CuO NPs as sustainable antibacterial nanomaterials and provide a basis for further investigation of their antibacterial mechanisms and safety [41-48]. Figure 12 presents the inhibition zone diameters (mm) of CG-CuO NPs against the tested bacterial strains.

Table 3. Inhibition zone diameters (mm) of CG-CuO NPs against the tested bacterial strains at different concentrations.

Type Bacterial / Concentration	Inhibition zone diameters (mm)			
	2.5 mg/mL	5 mg/mL	10 mg/mL	20 mg/mL
Salmonella tyhpi	20mm	20mm	20mm	20mm
Staphylococcus aureus	18mm	20mm	18mm	20mm
Escherichia coli	14mm	18mm	11mm	15mm

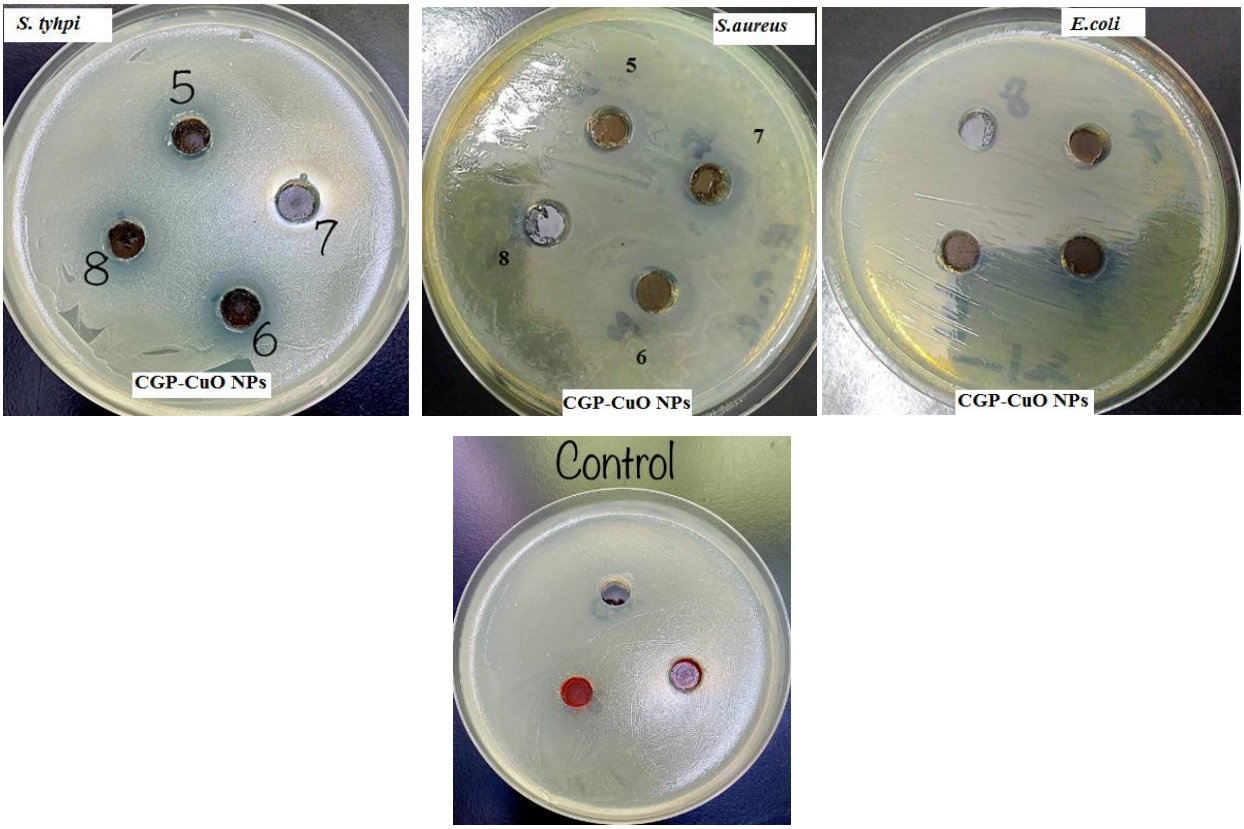

Fiq. 11. Shows the inhibition zone of (CG-CuO NPs) on bacterial isolates (5=20, 6=10, 7=5 and 8= 2.5) mg/ml, (control-DMSO).

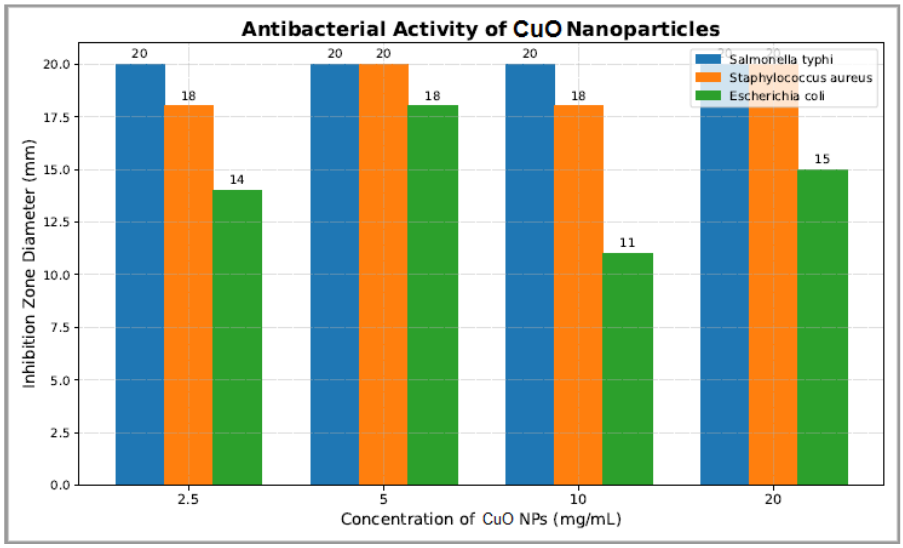

Fig.12. Bar graph showing concentration-dependent inhibition zones (mm) of (CG-CuO NPs).

5. Conclusions

This study demonstrates the feasibility of using *C. glomeruliflorus* aqueous extract as a biogenic medium for the green synthesis of copper oxide nanoparticles (CG-CuO NPs). Preliminary phytochemical screening revealed a diverse array of bioactive constituents, including phenols, alkaloids, flavonoids, anthraquinones, glycosides, saponins, terpenoids, steroids, carbohydrates, tannins, and coumarins, which may contribute to the reduction, nucleation, and stabilization of the resulting nanoparticles. The formation of CG-CuO NPs was initially indicated by the characteristic color change from blue to dark brown and was subsequently supported by UV–Vis, FTIR, XRD, SEM, and EDX analyses. UV–Vis spectroscopy revealed an absorption maximum at approximately 290 nm, corresponding to an estimated optical bandgap of 3.76 eV. FTIR analysis indicated the involvement of plant-derived functional groups, particularly those associated with hydroxyl, carbonyl, and aromatic moieties, in the interaction between phytochemical constituents and the nanoparticle surface. XRD confirmed the formation of predominantly phase-pure monoclinic CuO with a C2/c crystal structure. The calculated crystallite sizes ranged from 35.98 to 44.12 nm, with an average crystallite size of 40.97 nm, together with relatively low lattice microstrain and dislocation density. SEM revealed predominantly irregular to quasi-spherical nanoparticles with particle sizes of approximately 20–50 nm and moderate agglomeration. EDX confirmed Cu and O as the principal elemental constituents, with an atomic composition approaching the expected stoichiometry of CuO. Biological evaluation demonstrated that CG-CuO NPs exhibited antibacterial activity against both Gram-negative (*Salmonella typhi* and *Escherichia coli*) and Gram-positive (*Staphylococcus aureus*) bacteria. The maximum inhibition zones were 20 mm for *S. typhi* and *S. aureus* and 18 mm for *E. coli*. The antibacterial activity may arise from the combined effects of nanoscale surface interactions, copper ion-mediated effects, oxidative stress, and disruption of bacterial cell membranes; however,

these mechanisms require direct experimental verification. Overall, the findings identify *C. glomeruliflorus* as a previously unexplored and promising biogenic resource for the sustainable synthesis of CuO NPs. The integration of phytochemical-assisted synthesis with physicochemical characterization and antibacterial evaluation provides a foundation for further investigation of these nanoparticles. Future studies should focus on elucidating their antibacterial mechanisms, assessing cytotoxicity, biocompatibility, and in vivo safety, and optimizing synthesis conditions for reproducibility, scale-up, and potential biomedical or environmental applications.

Data availability statement

All data generated or analysed during this study are included in this published article [and its supplementary information files].

References

1. Worku LA. Green synthesis of zinc oxide nanoparticles using Rhus vulgaris fruit extract and zinc nitrate hexahydrate for photocatalytic, antioxidant, and antibacterial activities. Nanomaterials and Nanotechnology. 2026 Apr;16:18479804261441857. https://doi.org/10.1177/18479804261441857
2. Khadka D, Poudel BR, Bastakoti BP, Pokhrel MR. Green synthesis of CuO nanoparticles using Senegalia catechu bark, leaf, and stem: enhanced photocatalytic and antimicrobial activity. Next Materials. 2026 Apr 1;11:101960. https://doi.org/10.1016/j.nxmate.2026.101960
3. Al-Kazragi MA, Al-Heetimi DT, Al-Jaafari AK, Wilson LD. Green Synthesis of CuO Nanoparticles Using Beta vulgaris L. Extract for Removal of Methyl Violet Dye. The Scientific World Journal. 2026;2026(1):4954329. https://doi.org/10.1155/tswj/4954329
4. Lungu II, Stefanache A, Anton N, Lungu A, Platon VM, Mitran AM, Cioanca O, Mircea C, Hancianu M. Green-synthesized copper and copper oxide nanoparticles: Structural characterization and evaluation of biological activity. Antioxidants. 2026 Mar 7;15(3):339. https://doi.org/10.3390/antiox15030339
5. Olajesu MO, Abegunde SM. Ecofriendly synthesis and characterization of CuO nanoparticles from Blighia sapida pods for antimicrobial applications. Discover Chemistry. 2026 Jan 26;3(1):40. https://doi.org/10.1007/s44371-026-00501-2
6. Saleem MH, Ejaz U, Vithanage M, Bolan N, Siddique KH. Synthesis, characterization, and advanced sustainable applications of copper oxide nanoparticles: a review. Clean Technol Environ Policy, 2024;1–26. https://doi.org/10.1007/s10098-024-02774-6
7. Ahmed MH, Javed MT, Bahadur SUK, Tariq A, Tahir MH, Tariq ME, Ali MH. Antibacterial effects of copper oxide nanoparticles against E. coli induced infection in broilers. Appl Nanosci. 2022;12(7):2031–44. https://doi.org/10.1007/s13204-022-02482-x
8. Dadi R, Azouani R, Traore M, Mielcarek C, Kanaev A. Antibacterial activity of ZnO and CuO nanoparticles against gram positive and gram negative strains. Mater Sci Engineering: C. 2019;104:109968. https://doi.org/10.1016/j.msec.2019.109968
9. Athira K, Gurrala L, Kumar DVR. Biosurfactant-mediated biosynthesis of CuO nanoparticles and their antimicrobial activity. Appl Nanosci. 2021;11(4):1447–57. https://doi.org/10.1007/s13204-021-01766-y
10. Valadbeigi M, Mahmoudifard M, Ganji SM, Mehrabian S. Study on the antibacterial effect of CuO nanoparticles on Klebsiella pneumonia bacteria: efficient treatment for colorectal cancer. Biotechnol Appl Chem. 2023;70(6):1785–93. https://doi.org/10.1002/bab.2481

11. Bai B, Saranya S, Dheepaasri V, Muniasamy S, Alharbi NS, Selvaraj B, Gnanamangai BM. Biosynthesized copper oxide nanoparticles (CuO NPs) enhances the anti-biofilm efficacy against K. pneumoniae and S. aureus. J King Saud University- Science. 2022;34(6):102120.
12. Azizi H, Akbari N, Kheirandish F, Sepahvand A. Biogenic synthesized copper oxide nanoparticles by Bacillus subtilis: Investigating antibacterial activity on the mexAB-oprM efflux pump genes and cytotoxic effect on MCF-7 cells. Journal of Basic Microbiology. 2023 Sep;63(9):960-70. https://doi.org/10.1002/jobm.202200718
13. Saleh MM, Ali TM, Ali RM. Synthesis and characterization of copper oxide nanoparticles using Moringa Oleifera leaves Extract. University of Aden Journal of Natural and Applied Sciences. 2023 Oct 31;27(2):335-45. https://doi.org/10.47372/uajnas.2023.n2.a14
14. Anwaar S, Altaf F, Anwar T, Qureshi H, Siddiqi EH, Soufan W, Zaman W. Biogenic synthesis of copper oxide nanoparticles using Eucalyptus globulus leaf extract and its impact on germination and phytochemical composition of lactuca sativa.Sci Rep. 2024;14(1):1–15. https://doi.org/10.1038/s41598-024-78956-5
15. Afzal G, Jamal A, Kiran S, Mustafa G, Mehmood T, Ahmad F, Dawood S. Copper oxide nanoparticles synthesis using aerva Javanica and their antimicrobial activities. JAPS: J Anim Plant Sci, 2022;32(5). https://doi.org/10.36899/JAPS.2022.5.0547
16. Jabeen S, Siddiqui VU, Bala S, Mishra N, Mishra A, Lawrence R, Khan T. Biogenic synthesis of copper oxide nanoparticles from Aloe vera: antibacterial activity, molecular docking, and photocatalytic dye degradation. ACS Omega. 2024;9(28):30190–204. doi: 10.1021/acsomega.3c10179
17. Relhan A, Guleria S, Bhasin A, Mirza A, Zhou JL. Biosynthesized copper oxide nanoparticles by psidium Guajava plants with antibacterial, antidiabetic, antioxidant, and photocatalytic capacity. Biomass Convers Biorefinery, 2024;1–18. https://doi.org/10.1007/s13399-024-05544-y
18. Aswini R, Jothimani K, Kannan K, Pothu R, Shanmugam P, Boddula R, Al-Qahtani N. Carica Papaya leaf-infused metal oxide nanocomposite: a green approach towards water treatment and antibacterial applications. Environ Geochem Health. 2024;46(9):334. https://doi.org/10.1007/s10653-024-02090-4
19. ben Mosbah M, Alsukaibi AKD, Mechi L, Alimi F, Moussaoui Y. Ecological synthesis of CuO nanoparticles using Punica granatum L. peel extract for the retention of Methyl green. Water. 2022;14(9):1509. https://doi.org/10.3390/w14091509
20. Danışman-Kalındemirtaş F, Sert E, Tan E, Akyüz E, Karakuş S. Potential multifaceted applications of cisplatin-loaded camellia sinensis extract/CuO nanoparticles in cytotoxic and apoptotic effects. Biomass Convers Biorefinery. 2024;14(17):20261–73. https://doi.org/10.1007/s13399-023-04222-9
21. Thirunavukkarasu R, Nandhagopal M, Thirunavukkarasu S, Raji A, Kamath BR, Venkateswaran L. Ecosynthesis of copper and nickel oxide nanoparticles from Aegle marmelos extract: antimicrobial, antioxidant, and hemolytic activity evaluation. Materials Letters. 2025 Sep 15;395:138705. https://doi.org/10.1016/j.matlet.2025.138705
22. Velsankar KR, RM AK, Sudhahar S. Green synthesis of CuO nanoparticles via Allium sativum extract and its characterizations on antimicrobial, antioxidant, antilarvicidal activities. Journal of Environmental Chemical Engineering. 2020 Oct 1;8(5):104123. https://doi.org/10.1016/j.jece.2020.104123
23. Saleh MM, Saleh AL-Quhbi HA. Green synthesis and characterization of zinc oxide nanoparticles using Iphiona scabra DC. ex Decne leaf extract. Discover Applied Sciences. 2026 Aug 14. https://doi.org/10.1007/s42452-026-09306-5.

24. Bin-Asal FS, Saeed AA, Yahia AR. Corallocarpus glomeruliflorus: Pharmacological potential revealed by phytochemical and in silico investigations. Biochemistry and Biophysics Reports. 2025 Mar 1;41:101940. https://doi.org/10.1016/j.bbrep.2025.101940
25. Fioranelli M, Roccia MG, Flavin D, Cota L. Regulation of inflammatory reaction in health and disease. International Journal of Molecular Sciences. 2021 May 17;22(10):5277. https://doi.org/10.3390/ijms22105277
26. Ali DE, Gedaily RA, Ezzat SM, Sawy MA, Meselhy MR, Abdel-Sattar E. In silico and in vitro anti-inflammatory study of phenolic compounds isolated from Eucalyptus maculata resin. Scientific Reports. 2023 Feb 6;13(1):2093. https://doi.org/10.1038/s41598-023-28221-y
27. Devi A, Chaudhary A. Phytochemical-mediated green synthesis, mechanistic insights integrated with biological evaluation, density functional theory calculations and molecular docking studies of copper oxide nanoparticles. Scientific Reports. 2026 Jun 19;16(1):22697. https://doi.org/10.1038/s41598-026-58053-5.
28. Moroda MD, Deressa TL, Tiwikrama AH, Chala TF. Green synthesis of copper oxide nanoparticles using Rosmarinus officinalis leaf extract and evaluation of its antimicrobial activity. Next Materials. 2025 Apr 1;7:100337. https://doi.org/10.1016/j.nxmate.2024.100337
29. Belew AA, Assege MA, Belete AA, Muluneh EY, Gebremariam GN, Amera BD, Adugna AG, Legesse GA. Eco-friendly copper oxide nanoparticles (CuO NPs) synthesized from aqueous Arachis hypogaea seed extract with enhanced antioxidant and antibacterial activities. Results in Chemistry. 2026 Aug 18:103771. https://doi.org/10.1016/j.rechem.2026.103771
30. Aleman-Ramirez JL, Barragán-Trinidad M, Sebastián PJ, Okoye PU. Eco-engineered copper oxide nanoparticles using moringa oleifera pod's aqueous extract for biodiesel synthesis: green synthesis and process optimization. Biomass Futures. 2026 Apr 16:100043. 10.1016/j.bmf.2026.100043
31. Gebrie HT, Assege MA, Meshesha DS, Tebeje BA, Moges GW, Wodajo AT, Manahelohe GM, Belew AA. Biosynthesis and characterization of copper oxide nanoparticles from Plumbago zeylanica leaf extract for antibacterial and antioxidant activities. Scientific Reports. 2025 Aug 20;15(1):30656. https://doi.org/10.1038/s41598-025-10700-z
32. Ododo AG, Chinko BC, Dapper DV. Proximate analysis, phytochemical profiling and GC–MS characterization of bioactive compounds of ethanolic extract and oil of Arachis hypogaea. Discover Plants. 2026 Mar 2;3(1):46. https://doi.org/10.1007/s44372-026-00501-7
33. Buazar F, Sweidi S, Badri M, Kroushawi F. Biofabrication of highly pure copper oxide nanoparticles using wheat seed extract and their catalytic activity: A mechanistic approach. Green processing and synthesis. 2019 Jan 28;8(1):691-702. https://doi.org/10.1515/gps-2019-0040
34. Millavithanachchi SS, Gunasena MD, Galpaya GD, Priyadarshana HV, Indupama SV, Induranga DK, Kariyawasam WA, Kaluthanthri DV, Koswattage KR. Green synthesis, optimization, and characterization of CuO nanoparticles using Tithonia diversifolia leaf extract. Nanomaterials. 2025 Aug 6;15(15):1203. https://doi.org/10.3390/nano15151203
35. Aien J, Khan AA, Haq S, Khan AR, Elmnasri K, Ben Ali M, Al-Harbi MS, Alghonaim MI, Alsalamah SA, Qurtam AA, Boufahja F. Antibacterial, antioxidant and physicochemical properties of pipper nigram aided copper oxide nanoparticles. Crystals. 2023 Feb 15;13(2):330. https://doi.org/10.3390/cryst13020330

36. Abdullah H, Maqsood S, Zafar A, Ghuffar S. Biogenic synthesis of copper oxide nanoparticles using agro-waste extract and evaluation of their physicochemical properties. Phosphorus, Sulfur, and Silicon and the Related Elements. 2026 May 2:1-9. https://doi.org/10.1080/10426507.2026.2668511

37. Bayram D, Attar A, Yapaoz MA. Phytofabrication of copper oxide nanoparticles via Brassica napus L. var. napobrassica revealing mechanistic insights into ROS-induced antimicrobial and antibiofilm activity. Scientific Reports. 2026 Aug 20. https://doi.org/10.1038/s41598-026-67668-7

38. Saleh, M. M., Ba-Hamid, N. M., & Bamsaoud, S. F. (2026). Green Synthesis of CuO Nanoparticles Utilizing Moringa Oleifera Leaf Extract and Its Biological Applications. International Journal of Multidisciplinary Sciences and Advanced Technology Vol 7 No 2 (2026) 197–205.

39. Asemani M, Anarjan N. Green synthesis of copper oxide nanoparticles using Juglans regia leaf extract and assessment of their physico-chemical and biological properties. Green Processing and Synthesis. 2019 Jan 28;8(1):557-67. https://doi.org/10.1515/gps-2019-0025

40. Manik KH, Ahmed R, Habib MA, Nath A, Rhine A, Mim JJ, Islam S, Hossain N. Green synthesis and characterization of CuO nanoparticles using Acacia auriculiformis and Bauhinia variegata leaf extract for antibacterial applications. Next Materials. 2026 Jul 1;12:102009. https://doi.org/10.1016/j.nxmate.2026.102009

41. Vavilapalli SN, Rani SS, Mamidi G, Botsa SM. Green synthesis of CuO nanoparticles using Ixora chinesis leaf extract for photocatalytic decolourisation of Rhodamine B and antibacterial performance. Next Nanotechnology. 2026 Jun 1;9:100463. https://doi.org/10.1016/j.nxnano.2026.100463

42. Olajesu MO, Abegunde SM. Ecofriendly synthesis and characterization of CuO nanoparticles from Blighia sapida pods for antimicrobial applications. Discover Chemistry. 2026 Jan 26;3(1):40. https://doi.org/10.1007/s44371-026-00501-2

43. Kalaiyan G, Suresh S, Prabu KM, Thambidurai S, Kandasamy M, Pugazhenthiran N, Kumar SK, Muneeswaran T. Bactericidal activity of Moringa oleifera leaf extract assisted green synthesis of hierarchical copper oxide microspheres against pathogenic bacterial strains. Journal of Environmental Chemical Engineering. 2021 Feb 1;9(1):104847.https://doi.org/10.1016/j.jece.2020.104847

44. Ali SS, Dharmadhikari K, Saiyed KI, Vasava H, Jowhari MA, Robin P. Ecofriendly synthesis of silver nanoparticles using Barleria gibsonii and evaluation of antibacterial antioxidant cytotoxic and catalytic activities. Scientific Reports. 2026 Feb 11;16(1):8281. https://doi.org/10.1038/s41598-026-37330-3

45. Ben Cheikh C, Nedjimi MS, Ouahrani MR, Belkhelfa H, Dizge N. Ephedra alata aqueous extract mediated green synthesis of CuO nanoparticles and their antioxidant, antidiabetic, and antibacterial properties. International Journal of Environmental Science and Technology. 2026 Jun;23(6):429. https://doi.org/10.1007/s13762-026-07229-7

46. Getachew AM, Bacha EG, Geleta WS. Statistical optimization of eco-friendly synthesized silver nanoparticles using Discopodium penninervium Hochst leaf extract for enhanced antimicrobial efficacy. Scientific Reports. 2025 Nov 22;15(1):45017. https://doi.org/10.1038/s41598-025-29253-2

47. Deo, R., Apta, D., & Devi, M. (2026). CuO Nanoparticles for Effective Photocatalytic Methylene Blue Dye Degradation: Kinetic, Thermodynamic, and Mechanistic Role of Reactive Species. *ChemistrySelect*, *11*(19), e73458. https://doi.org/10.1002/slct.73458

48. Aysha M, Selvam K, Adhavan R, Prakash P, Shivakumar MS. Green synthesis of copper oxide nanoparticles using Dolichandrone falcata (Wall. ex DC.) Seem. leaf extract and assessment of antioxidant, antimicrobial, anti-diabetic and anticancer potentials. Applied Biochemistry and Biotechnology. 2025 Oct;197(10):6722-40. https://doi.org/10.1007/s12010-025-05356-4

Acknowledgments

The author expresses sincere gratitude to Dr. Nabil AL-Hudaifi (Department of Marine Pollution Laboratory, Faculty of Sciences Environmental, Hadhramout University) for providing access to the UV–Vis spectrophotometer. Thanks are also extended to the Supreme Authority for Drugs and Metrology (Aden Branch, Yemen) for granting access to the FTIR instrument, and to the Laboratory of Nano Chemistry and Nano Electrochemistry (Nalchik University, Russian Federation) for providing access to the SEM-EDX and XRD instruments.

Author contributions

M. M. A. S.: conceptualized and designed the study, performed the experiments, analyzed the data, wrote the original draft, and reviewed and edited the manuscript. The author approved the final version.

Funding

This study did not receive any funding.

Declarations

Competing interests

The author declares no competing interests.

Ethics approval and consent to participate

This article does not contain any studies on human or animal subjects. The current experimental research and field study, including the collection of plant material, complies with relevant institutional, national, and international guidelines and legislation and is used for research and development.